Multiphysics Modeling of Radiofrequency Heating of Carbon Fiber Composites

Rohith Premanandan

A thesis
submitted in partial fulfillment of the requirements for the degree of

Master of Science

University of Washington

2024

Reading Committee:

Aniruddh Vashisth, Chair

Ashis Banerjee

Vipin Kumar

Program Authorized to Offer Degree:
Mechanical Engineering

University of Washington

Abstract

Multiphysics Modeling of Radiofrequency Heating of Carbon Fiber Composites

Rohith Premanandan

Chair of the Supervisory Committee:
Aniruddh Vashisth
Department of Mechanical Engineering

Radiofrequency (RF) heating has become a vital technique in processing carbon fiber composites, especially for high-performance applications like aerospace. To understand how RF heating impacts these materials, we need to look at the interplay between electromagnetic fields, heat transfer, and mechanical stresses. Our research aims to create a detailed model that captures these interactions and accurately predicts temperature changes and mechanical responses in the composite material. Using established theories and validating our model through analytical solutions and finite element analysis (FEA), we aim to understand the effects of varying RF power, the role of carbon black fillers, and how the temperature-dependent behavior of epoxy resin impacts the process. By doing so, we hope to optimize material choices and ensure the stability and reliability of these composites in advanced manufacturing.

TABLE OF CONTENTS

Page

List of Figures ii

Chapter 1: Introduction 1
1.1 Background and Motivation 1
1.2 Literature Review and Related Work 2

Chapter 2: Thermoelastic Model 3
2.1 Formulation of the Thermoelastic Model 3
2.2 Solution of the Thermoelastic Model 6
2.3 FEA Validation of the Thermoelastic Model 8

Chapter 3: Parametric Study of the Thermoelastic Model 11
3.1 Variation of Input power 11
3.2 Introduction of Carbon Black filler 13
3.3 Temperature Dependent Behavior of Epoxy Resin 18
3.4 Conclusion 22
3.5 Future Work 22

Bibliography 24

Appendix A: Where to find the files 25

LIST OF FIGURES

Figure Number Page

2.1 Geometry of the thermoelastic model 3
2.2 $w(x,t)$ contour at along the spatial direction x of the microbeam at 50 W input power 7
2.3 $T(x,t)$ contour at along the spatial direction x of the microbeam at 50 W input power 8
2.4 $w(x,t)$ observed in FEA at 50 W input heat flux after 1 s 9
2.5 $T(x,t)$ observed in FEA at 50 W input heat flux after 1 s 10

3.1 $w(x,t)$ and $T(x,t)$ at different powers 11
3.2 Maximum value of $w(x,t)$ from simulation with varying input power 12
3.3 Maximum value of $T(x,t)$ from simulation with varying input power 13
3.4 $w(x,t)$ with varying filler content 15
3.5 $T(x,t)$ with varying filler content 16
3.6 Maximum value $w(x,t)$ from simulation with varying filler content 17
3.7 Maximum value of $T(x,t)$ from simulation with varying filler content 17
3.8 Variation of thermal expansion coefficient of epoxy resin at different temperatures [1] 20
3.9 Deflection $w(x,t)$ with varying temperature properties at 50 W 21
3.10 Temperature distribution in FEA with varying temperature properties at 50 W 21

ACKNOWLEDGMENTS

I would like to express my heartfelt gratitude to Dr. Aniruddh Vashisth for his mentorship and guidance, and to my committee members Dr. Ashis Banerjee and Dr. Vipin Kumar for their valuable insights and support throughout this project. My sincere thanks to Surabhit Gupta for his valuable inputs. I would also like to thank my parents for their continued support throughout my academic journey.

DEDICATION

to my parents

Chapter 1

INTRODUCTION

1.1 Background and Motivation

In the field of materials science and engineering, understanding the complex interplay of various physical phenomena is critical for developing accurate predictive models and ensuring structural component reliability. Understanding these complex interactions is critical, especially in composite materials where multiple factors such as electromagnetic fields, heat transfer, and structural mechanics all come together.

One important aspect of this complexity is predicting the temperature distribution within composite materials as they are exposed to various external factors, such as induced currents or thermal loads. As these materials heat up, temperature distribution throughout the structure is critical to its overall performance and longevity. However, accurately modeling this temperature distribution necessitates taking into account the complex interaction of electromagnetic fields, heat transfer mechanisms, and the material's structural response.

Furthermore, understanding how composite materials mechanically respond to thermal stresses is critical for avoiding damage or failure in operational environments. Thermal stresses caused by temperature gradients within a material can cause deformation, delamination, or even catastrophic failure if not managed correctly. Thus, developing comprehensive models that incorporate thermal, and structural considerations is critical for ensuring the reliability and durability of composite structures in a variety of applications.

This work is motivated by the need to improve our understanding of these complex interactions and developing sophisticated computational tools capable of predicting the behavior of composite materials under a variety of operating conditions.We hope to provide useful insights for the design, optimization, and performance assessment of composite structures in a variety of industries, including aerospace, automotive, and renewable energy. Finally, we hope to contribute to the development of more dependable, efficient, and long-lasting

materials and structures that meet the demands of contemporary engineering challenges.

1.2 Literature Review and Related Work

One key aspect of this complexity is predicting the temperature distribution within composite materials subjected to external factors like induced currents or thermal loads. Accurate temperature distribution modeling is vital as it significantly impacts the material's overall performance and longevity. For example, Zhang and Liu (2017)[2] explored the multiphysics modeling of heat transfer and thermal stress in composite structures, highlighting the necessity of integrating thermal and structural analyses for better predictive accuracy.Understanding how composite materials respond mechanically to thermal stresses is critical for avoiding damage or failure. Thermal stresses from temperature gradients can result in deformation, delamination, or catastrophic failure. Chen and Yuan (2020)[3] conducted a review of coupled electromagnetic, thermal, and structural analysis of composite structures, emphasizing the importance of comprehensive models that integrate these aspects to ensure structural reliability. Wang, Li, and Huang (2018)[4] gave a thorough overview of multiphysics modeling approaches for studying the coupled behavior of electromagnetic, thermal, and mechanical phenomena in composites. Their work emphasizes the benefits of incorporating multiple physical phenomena into a single model for enhanced predictive capabilities.

Overall, these studies show significant progress in understanding and modeling the complex interactions found in composite materials. Researchers have developed tools that provide valuable insights into the behavior of composite structures under a variety of operating conditions by incorporating multiple physical phenomena into comprehensive multiphysical models. This research is critical for advancing the design, optimization, and performance assessment of composite materials in a variety of engineering fields that employ RF fields.

Chapter 2

THERMOELASTIC MODEL

2.1 Formulation of the Thermoelastic Model

The response of the thermoelastic microbeam due to Radio Frequency (RF) heating is inspired from [5] , the previous solutions of thermoelastic models the experiments performed in the lab.

Consider a homogeneous, isotropic thermally dependent composite structure. The mechanical and thermal properties assumed in the structure are listed in the table.This structure is shaped like a rectangular beam with specific dimensions length = L ($0 \leq x \leq L$),width=a ($-a/2 \leq y \leq a/2$) and thickness=h ($-h/2 \leq z \leq h/2$) in a cartersian coordinate system Oxyz as shown in Fig. 2.1. We assume that the microbeam undergoes bending

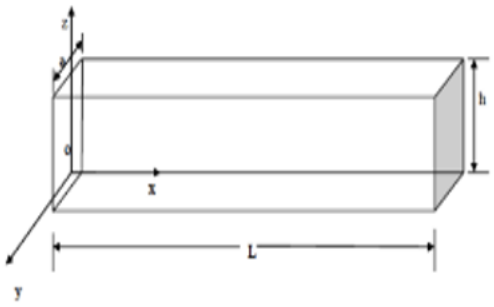

Figure 2.1: Geometry of the thermoelastic model

vibrations of small amplitude about the x-axis so that the deflection is consistent with the linear Euler- Bernoulli theory. Hence the displacements of the microbeam can be written

as

$$\begin{aligned} u_1 = u &= -z\frac{\partial w}{\partial x}, \\ u_2 &= 0, \\ u_3 &= w(x,t), \end{aligned} \tag{2.1}$$

where w is the lateral deflection and u is the axial displacement.

The equation that describes the motion of the beam during its free flexural vibrations is given by

$$\frac{\partial^2 M}{\partial x^2} + \rho A\left(\frac{\partial^2 w}{\partial t^2}\right) = 0, \tag{2.2}$$

where $A = ah$ is the cross-sectional area and M is the flexural moment of the microbeam's cross section. The expression for the flexural moment of the beam's cross section is given by

$$M(x,t) = -a\int_{-h/2}^{h/2} t_x z\, dz = (\lambda + 2\mu) I\frac{\partial^2 w}{\partial x^2} + M_T, \tag{2.3}$$

where λ and μ are Lame's constants and$I = ah^3/12$ is the moment of inertia of the cross section; M_T is the thermal moment of the beam given by

$$M_T = \beta\int_{-h/2}^{h/2} aTz\, dz. \tag{2.4}$$

where $\beta = (3\lambda + 2\mu)\alpha_t$; α_t is the linear thermal expansion; T is the temperature change measured from the absolute temperature T_0 ($T_0 \neq 0$).

Substituting Eq.(2.4) in Eq.(2.3) we get the following eqaution of motion of the microbeam:

$$(\lambda + 2\mu) I\frac{\partial^4 w}{\partial x^4} + \rho A\left(\frac{\partial^2 w}{\partial t^2}\right) + \frac{\partial^2 M_T}{\partial x^2} = 0. \tag{2.5}$$

To model the heat conduction induced by the RF pulse A wave-form thermal equation was presented by Lord and Shulman (LS) was used.The LS model is a thermoelasticity theory that incorporates a hyperbolic heat transfer equation derived by modifying Fourier's heat conduction law. The authors introduced the concept of relaxation time. According to their theory, the linear relationship between temperature and heat flux incorporates both the rate of temperature change and thermal rates. [6].The heat transfer equation is hence represented as

$$\left(1+\tau_0\frac{\partial}{\partial t}\right)\left(\beta T_0\dot{u}_{i,j}+\rho C^*\dot{T}-Q\right)=K^*\nabla^2 T, \tag{2.6}$$

where $K*$ is the coefficient of thermal conductivity; τ_0 is the thermal relaxation time of the heat expressed as the lag time required to construct the steady condition of the heat conduction as a gradient of temperature; Q is the constant heat source; $C*$ is the specific heat at constant strain; u_i is the displacement components.

Eq.(2.6) with the aid of Eq.(2.1) can be written as

$$K^*\left(\frac{\partial^2 T}{\partial x^2}+\frac{\partial^2 T}{\partial z^2}\right)=\left(1+\tau_0\frac{\partial}{\partial t}\right)\left[-\beta T_0 z\frac{\partial}{\partial t}\left(\frac{\partial^2 w}{\partial x^2}\right)+\rho C^*\dot{T}-Q\right]. \tag{2.7}$$

The initial temperature distribution $T(x,z,0)=T_0$. For $t=0$, the upper surface, $z=h$, of the beam is heated uniformly by a laser pulse.

The initial conditions of the problem are assumed to be homogeneous as shown below

$$w(x,t)\Big|_{t=0}=\frac{\partial w(x,t)}{\partial t}\Big|_{t=0}=0 \tag{2.8}$$

$$\frac{\partial T(x,t)}{\partial t}\Big|_{t=0}=0 \tag{2.9}$$

$$T(x,t)\Big|_{t=0}=T_0 \tag{2.10}$$

These initial conditions are further defined by the assumption that both ends of the microbeam are clamped and maintained at a constant temperature, with no variation in the volume fraction fields.. Mathematically, it can be written as

$$w(x,t)\Big|_{x=0,L}=\frac{\partial w(x,t)}{\partial x}\Big|_{x=0,L}=0 \tag{2.11}$$

$$T(x,t)\Big|_{x=0,L}=T_0 \tag{2.12}$$

2.2 Solution of the Thermoelastic Model

In order to solve set of coupled partial differential equations (PDEs) that describe the thermoelastic behavior of a microbeam we have used Python 3.10.12.The code utilizes several numerical methods to solve the coupled partial differential equations (PDEs) governing the thermoelastic behavior of a microbeam

2.2.1 Finite Difference Method (FDM) for Spatial Discretization

The Finite Difference Method (FDM) is a numerical technique used to approximate solutions to differential equations by discretizing the spatial domain. This method is particularly useful for solving partial differential equations (PDEs) where analytical solutions are challenging or impossible to obtain. In this context, we apply FDM to discretize the spatial domain of a microbeam for the purpose of solving the governing PDEs.

For a function $u(x)$ defined at discrete points, the second-order central difference approximation for the second derivative is given by:

$$\frac{\partial^2 u}{\partial x^2} \approx \frac{u_{i+1} - 2u_i + u_{i-1}}{(\Delta x)^2} \tag{2.13}$$

2.2.2 Ordinary Differential Equation (ODE) Solver for Time Integration

To track how the system evolves over time, we use a powerful tool from the SciPy library called *solve_ivp*. This tool is designed to solve systems of equations that describe how things change over time, known as ordinary differential equations (ODEs). For time integration, the solver $RK45$ is employed.$RK45$ is a member of the Runge-Kutta family of methods and is specifically an adaptive method of order 5(4). This means it uses a fifth-order accurate method to estimate the solution but also provides a fourth-order accurate method to control the error.

We start by converting our original set of partial differential equations (PDEs) into ODEs. This is done by breaking down the spatial component into small steps using a technique called finite differences. Once we have our ODEs, *solve_ivp* takes over, solving these equations over the time interval we're interested in, from the initial time $t = 0$ to some final time $t = t\_final$.The use of RK45 ensures that the integration is both accurate

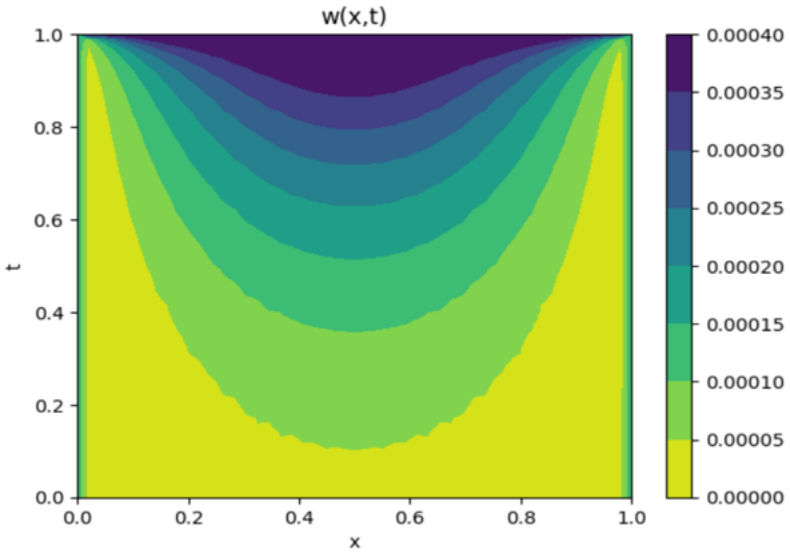

Figure 2.2: $w(x,t)$ contour at along the spatial direction x of the microbeam at 50 W input power

and computationally efficient, making it suitable for complex, coupled systems like the one under study. .

2.2.3 Analysis of Lateral Displacement Profile $w(x,t)$

The contour plots provide insight into how the lateral deflection $w(x,t)$ changes over both the spatial variable x and the temporal variable t as shown below . Notably, the boundaries at $x = 0$ and $x = 1$ exhibit lower displacement values in comparison to the midpoint at $x = 0.5$. This indicates that the deflection is more pronounced in the central region of the micro beam.

2.2.4 Analysis of Temperature Profile $T(x,t)$

Regarding the temperature profile $T(x,t)$, the temperature distribution appears relatively uniform along the spatial axis x at any given time t.The temperature profile T(x,T) can be represented in the contour plot as shown below.

Initially, at $t = 0$, the temperature is uniformly lower across the entire spatial domain.

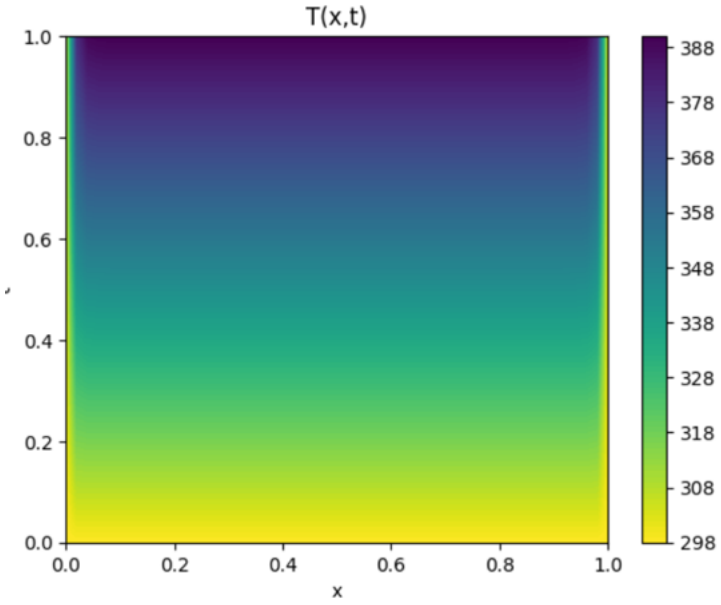

Figure 2.3: $T(x,t)$ contour at along the spatial direction x of the microbeam at 50 W input power

As time progresses and approaches $t = 1$ second, the temperature increases. The highest temperature values are observed at the upper regions of the plot, indicating that heat accumulates more in these areas over time. This temporal increase in temperature suggests a dynamic heating process where thermal energy distribution changes significantly within the first second.

2.3 FEA Validation of the Thermoelastic Model

To validate the accuracy of the results from the proposed model we have used Finite Element Analysis (FEA) . The FEA was performed in Abaqus/Standard 2022.

In Abaqus 2022, a coupled temperature-displacement analysis was performed that involves simultaneously solving for temperature and displacement fields within a structure, taking into account the interactions between thermal and mechanical behaviors. To perform this analysis, we start by defining the problem's geometry and material properties, including thermal conductivity, specific heat, density, elastic modulus, Poisson's ratio, and

the coefficient of thermal expansion. The same material properties were used as used in the code to generate the results for the thermoelastic model.

We apply different thermal loads (surface heat flux) to analyze its effect on the microbeam. As described in the formulation of thermoelastic model , the two ends of the micro beam are clamped using the ENCASTRE boundary condition which refers to a boundary condition that fully constrains the surface, preventing any translation or rotation in all 3 axis.

The results are visualized using the Abaqus 2022 Visualization module, allowing examination of temperature distributions, displacement field.

2.3.1 FEA Validation of Lateral Displacement $w(x,t)$

The lateral deflection pattern $w(x,t)$ results from FEA exhibit the characteristic pattern as shown below.

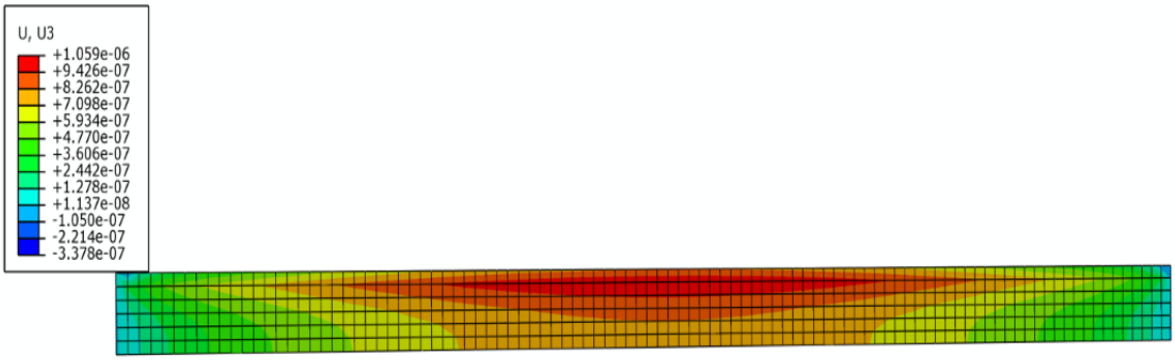

Figure 2.4: $w(x,t)$ observed in FEA at 50 W input heat flux after 1 s

After comparing the results we can conclude that that both the computational code and FEA exhibit the same characteristic pattern for $w(x,t)$ at same power. Both methods show that the deflection is highest at the midpoint of the beam. As expected, the deflection reduces towards the supports. The computational code and FEA both demonstrate this trend, confirming the theoretical prediction that the bending moment, and thus the

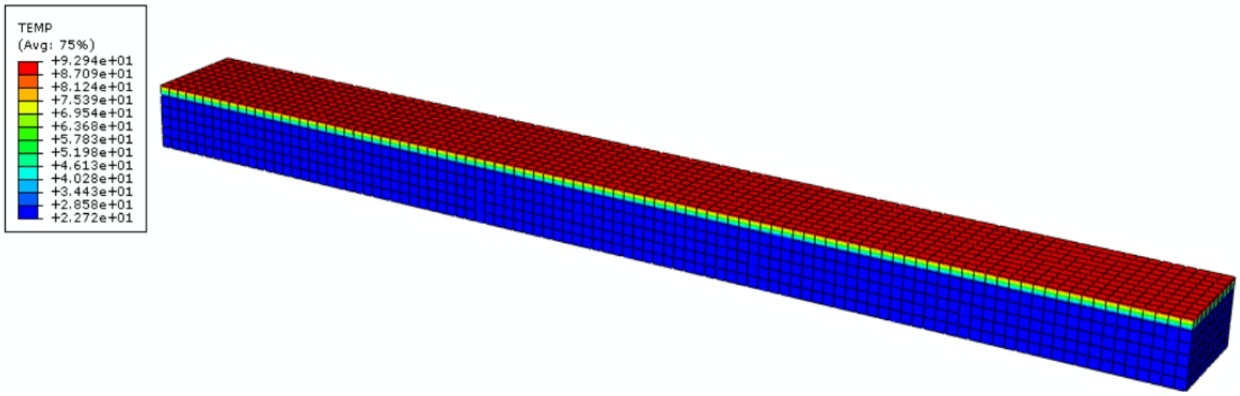

Figure 2.5: $T(x,t)$ observed in FEA at 50 W input heat flux after 1 s

deflection, is minimal at the supports.

2.3.2 FEA Validation of Temperature Profile $T(x,t)$

The temperature profile $T(x,t)$ obtained from FEA is shown in Figure 3.7. In our experiments, the bar was maintained at an ambient temperature of 25°C. This baseline condition was consistently used for all measurements, ensuring a stable reference point for evaluating temperature changes induced by applied power

In our experiments, the bar was maintained at an ambient temperature of 25°C. This baseline condition was consistently used for all measurements, ensuring a stable reference point for evaluating temperature changes induced by applied power

The temperature distribution along the length of the structure was observed to be uniform in the longitudinal direction.At an input power of 50 W, the observed temperature increased to 92.4°C. The pattern observed in our FEA simulations closely matched the pattern predicted by our computational code.

Chapter 3

PARAMETRIC STUDY OF THE THERMOELASTIC MODEL

3.1 Variation of Input power

The input power was increased from 10 W to 100 W to observe the effect on $w(x,t)$ and $T(x,t)$.

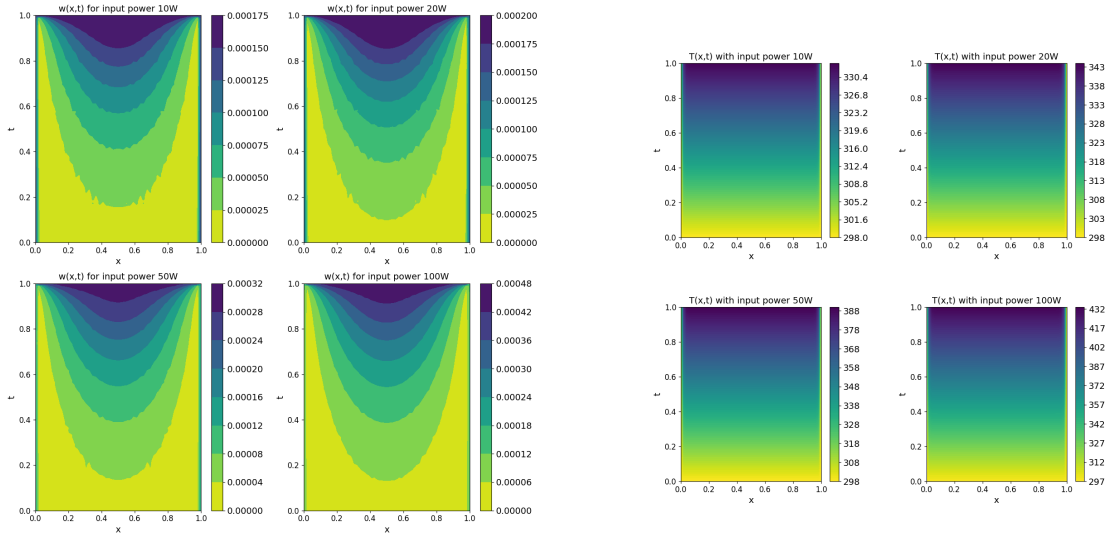

(a) $w(x,t)$ at different powers

(b) $T(x,t)$ at different powers

Figure 3.1: $w(x,t)$ and $T(x,t)$ at different powers

As the input power increases, the maximum value of the deflection, $w(x,t)$, also increases. This trend is observed due to the direct relationship between the input power and the thermal energy generated within the composite material. Higher input power results in greater heat generation, leading to increased temperatures throughout the material. The elevated temperatures cause the material to expand more, which in turn increases the deflection observed.

As the input power increases, the maximum temperature achieved in the material also rises. Higher input power provides more energy per unit time, causing the material to heat up more rapidly and reach higher temperatures.The temperature gradient over time becomes steeper with increasing input power, indicating a faster rate of heating. This steeper gradient means that the temperature rises more quickly when higher power is applied.

Besides we also compared the results with the FEA simulation and observed the similar trend as observed from the code. The plots for input power vs maximum magnitude of $w(x,t)$ and maximum magnitude of $T(x,t)$ at different powers are given below.

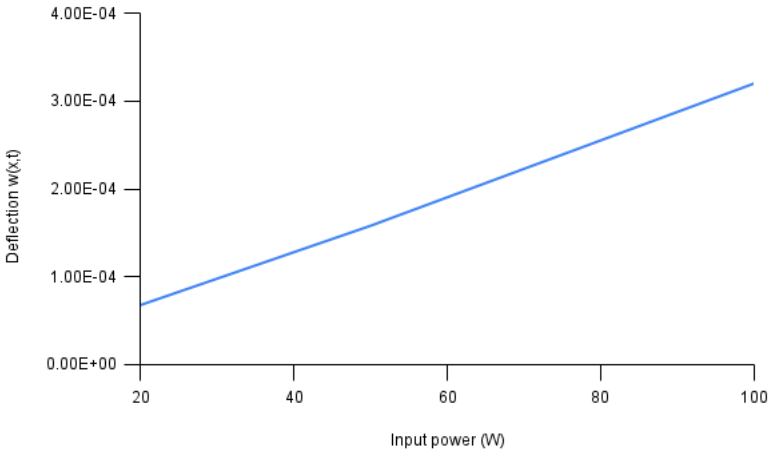

Figure 3.2: Maximum value of $w(x,t)$ from simulation with varying input power

The importance of varying power inputs is that it helps us simulate the real-world conditions composite materials face, where thermal loads constantly change. This variability is essential for truly understanding how these materials perform under different stresses and ensuring they remain reliable across various scenarios. By studying how different power levels affect these materials, we can predict and prevent potential failures, making sure our designs are safe and effective.

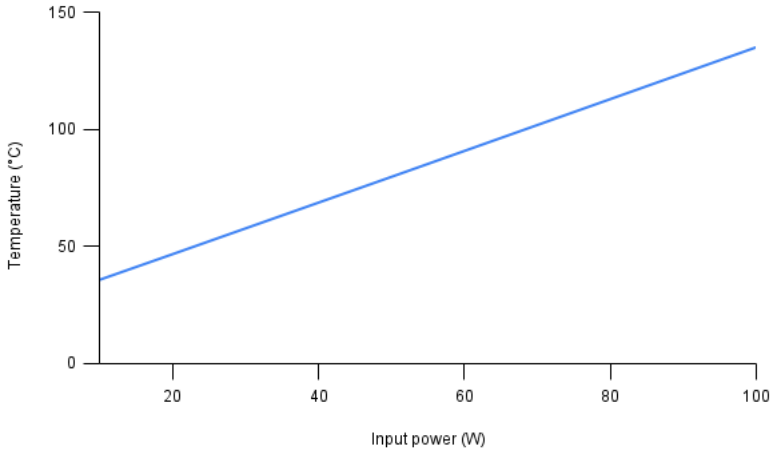

Figure 3.3: Maximum value of $T(x,t)$ from simulation with varying input power

3.2 Introduction of Carbon Black filler

Numerous researchers are exploring the impact of various particulates or fillers added to composite materials. This study examines how different quantities of carbon black particulates influence the mechanical performance of carbon fiber-reinforced epoxy composites. Increases of 65.78%, 32.07%, and 36.11% in tensile strength, flexural strength, and impact strength, respectively, have been observed in the hybrid composite (containing 10 wt% carbon black) compared to the conventional carbon fiber-reinforced epoxy composite [7].

Five batches with CB/epoxy weight ratios of 4/6, 5/5, 6/4, 6.5/3.5, and 7/3 were prepared, labeled as F4/6, F5/5, F6/4, F6.5/3.5, and F7/3, respectively. It was observed that all samples exhibited a significant increase in thermal conductivity values as the CB content increased[8].

Hence in our study we have increased the carbon filler content from 0%- 30% to observe the effect on $w(x,t)$ and $T(x,t)$. The mechanical properties such as Young's Modulus E and Poisson's ratio ν, and thermal properties such as thermal expansion coefficient α and thermal conductivity K of the composite with CB are calculated using the rule of mixtures, where carbon black and carbon fiber epoxy resin composite are the constituents of the

composite. The formulas are as follows:

- Young's Modulus E

$$E_c = V_{CB}E_{CB} + (1 - V_{CB})E_{CFRP}$$

- Poisson's Ratio ν

$$\nu_c = V_{CB}\nu_{CB} + (1 - V_{CB})\nu_{CFRP}$$

- Thermal Expansion Coefficient α

$$\alpha_c = V_{CB}\alpha_{CB} + (1 - V_{CB})\alpha_{CFRP}$$

- Thermal Conductivity K

$$K_c = V_{CB}K_{CB} + (1 - V_{CB})K_{CFRP}$$

where:

- E_c, ν_c, α_c, and K_c are the Young's Modulus, Poisson's ratio, thermal expansion coefficient, and thermal conductivity of the composite.

- E_{CB} and E_{CFRP} are the Young's Moduli of carbon black and the carbon fiber epoxy resin composite, respectively.

- ν_{CB} and ν_{CFRP} are the Poisson's ratios of carbon black and the carbon fiber epoxy resin composite, respectively.

- α_{CB} and α_{CFRP} are the thermal expansion coefficients of carbon black and the carbon fiber epoxy resin composite, respectively.

- K_{CB} and K_{CFRP} are the thermal conductivities of carbon black and the carbon fiber epoxy resin composite, respectively.

- V_{CB} is the volume fraction of carbon black, and $1 - V_{CB}$ is the volume fraction of the carbon fiber epoxy resin composite.

Filler Content	$E(GPa)$	ν	$\alpha(K^{-1})(\times 10^{-6})$	$K(W/m \cdot K)$
0	70	0.282	21.3	5.64
0.05	71	0.2839	20.46	9.885
0.1	71.5	0.2848	19.62	14.076
0.2	72	0.2856	17.94	22.512
0.3	73	0.2874	16.26	30.948

Table 3.1: Mechanical and Thermal Properties of the composite with different filler content

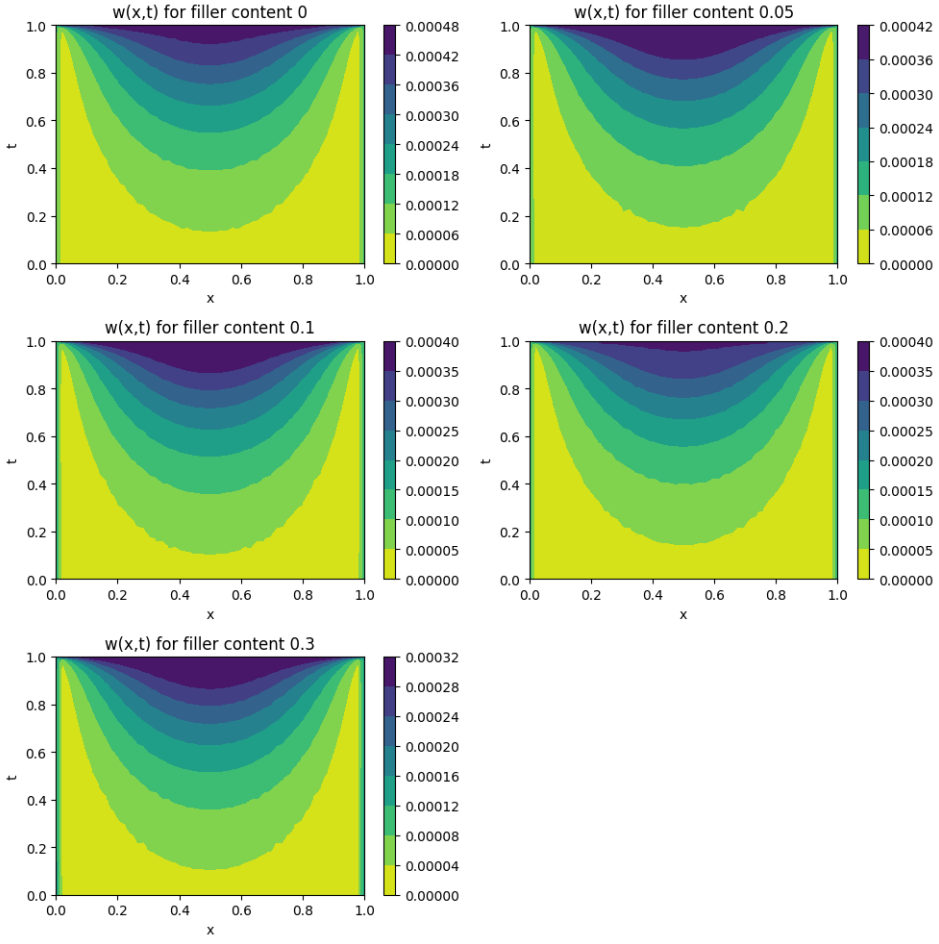

Figure 3.4: $w(x,t)$ with varying filler content

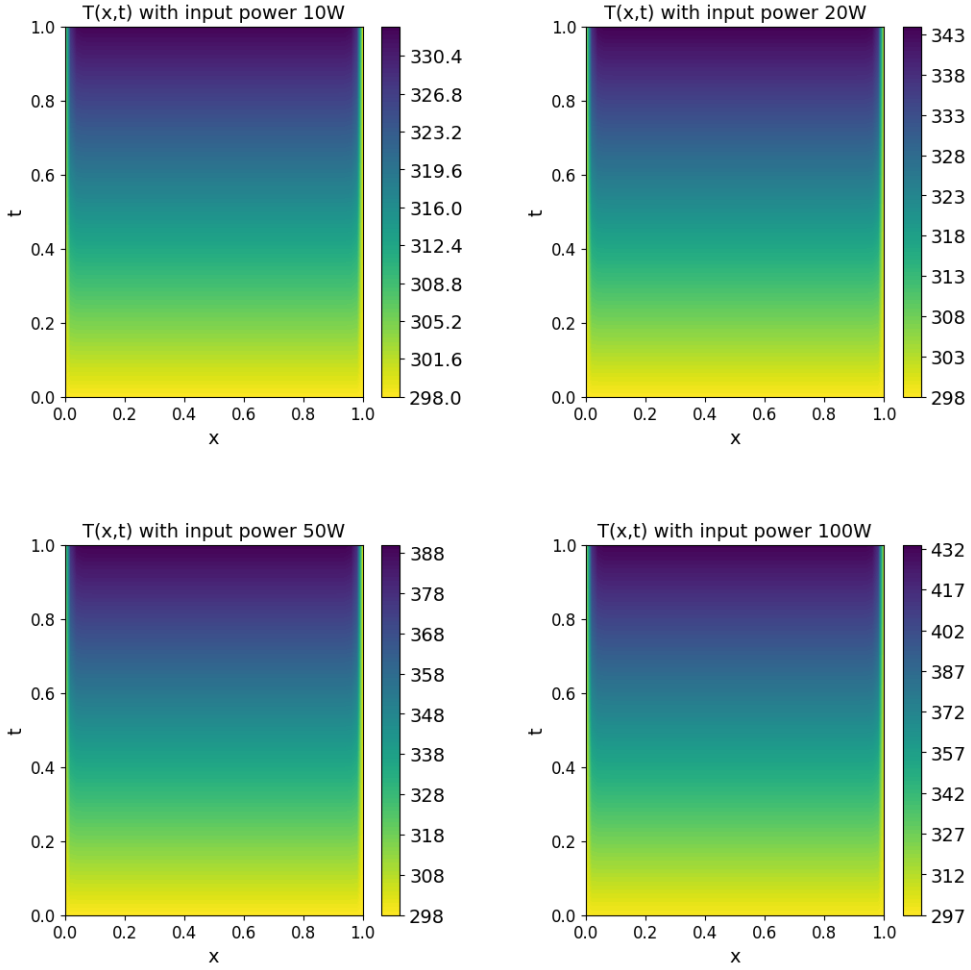

Figure 3.5: $T(x,t)$ with varying filler content

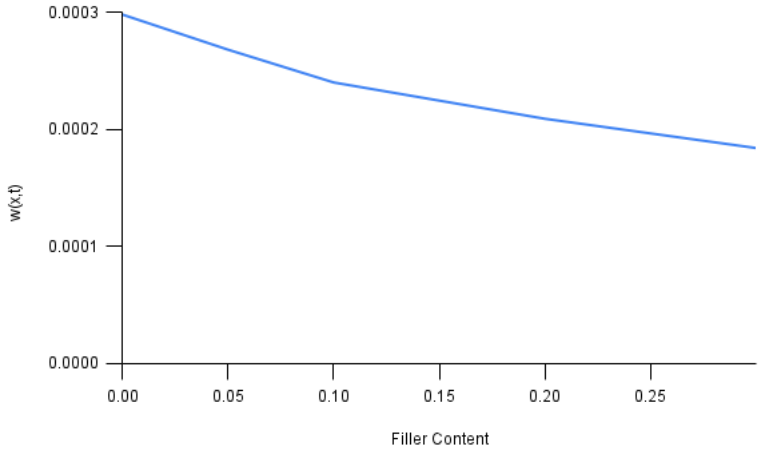

Figure 3.6: Maximum value $w(x,t)$ from simulation with varying filler content

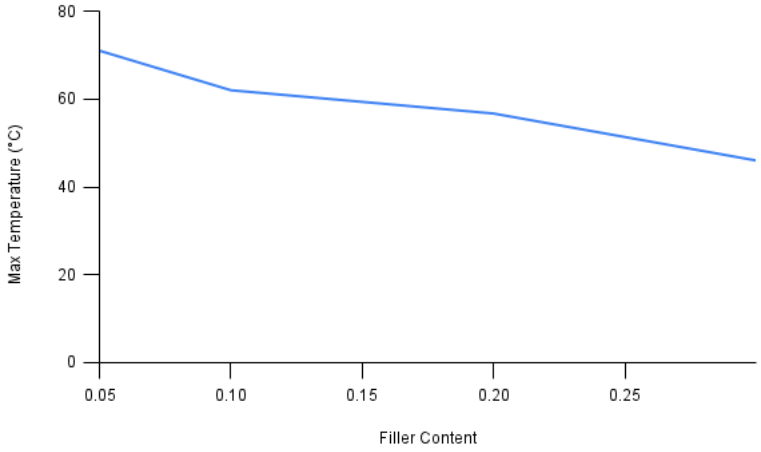

Figure 3.7: Maximum value of $T(x,t)$ from simulation with varying filler content

The input power was kept at 50 W and filler content was increased to observe the effect on $w(x,t)$ and $T(x,t)$. The contours below represent the variation of $w(x,t)$ and $T(x,t)$ as shown in Fig.3.4 and Fig.3.5. Once we executed the code we have performed FEM to compare the results. Our analysis shows that as filler content increased the maximum tem-

perature and deflection of the composite decreased as shown in Fig.3.6 and Fig. 3.7.

As the filler content increases, the overall displacement of the composite material decreases.The decrease in displacement with increasing filler content can be attributed to the enhanced stiffness (modulus) of the composite.Carbon black, known for its high modulus, imparts rigidity to the composite matrix.Higher filler content results in composites with increased stiffness, making them suitable for applications requiring high rigidity and minimal deformation. This property is particularly beneficial in structural applications where maintaining dimensional stability under mechanical loads is critical, such as in aerospace, automotive, and construction sectors.

As the filler content increases, the maximum temperature within the composite decreases due to higher overall thermal conductivity.The addition of carbon black, which has higher thermal conductivity compared to the epoxy resin, enhances the composite's overall ability to dissipate heat.he resulting lower operational temperatures contribute to improved performance, reliability, and extended service life of materials, particularly in electronics, thermal management, and high-temperature settings

In conclusion, increasing filler content in composite materials, particularly with the addition of high-modulus fillers like carbon black, leads to enhanced stiffness and reduced displacement. This property is advantageous in structural applications where dimensional stability under mechanical loads is crucial, such as in aerospace, automotive, and construction sectors.

One potential application for composites with increased filler content and improved thermal conductivity could be in the development of heat sinks for electronic devices. These composites could effectively dissipate heat away from sensitive electronic components, ensuring optimal performance and reliability even in demanding thermal environment.

3.3 Temperature Dependent Behavior of Epoxy Resin

The mechanical and thermal properties of composite materials are crucial factors in determining their suitability for various applications, especially when subjected to fluctuating temperatures. The mechanical properties such as Young's Modulus E and Poisson's ratio

ν, and thermal properties such as thermal expansion coefficient α and thermal conductivity K of the epoxy resin hence do not remain constant and its affect is observed in the analysis

The following relations have been used to take into account the temperature dependant mechanical and thermal properties of epoxy resin. Once these properties are known then rule of mixtures has been used to calculate the combined property (Assuming 40% Epoxy resin and 60 % Carbon fiber). The temperature was increased from 0°C to 80 °C with increments of 20 °C

The relation between Young's modulus (E) and temperature, derived from the third law of thermodynamics, is given by the equation:

$$E = E_0 - BT \exp\left(-\frac{T_M}{T}\right) \tag{3.1}$$

In this equation: E_0 represents the Young's modulus at 0 Kelvin. T is the absolute temperature. B is a material-dependent parameter, linked to Gruneisen's constant (γ), which characterizes the slope of the Young's modulus-temperature curve and decreases from a constant value as temperature decreases. The term $\exp\left(-\frac{T_M}{T}\right)$ is a single Boltzmann factor, where T_M is another material-dependent parameter correlated with the Debye temperature (Θ). γ and Θ are associated with the volume thermal expansion and specific heat, respectively. The Poisson's ratio ν at different temperatures has been extracted from [1].

The thermal expansion coefficient α at different temperatures has been extracted from the plot given in Fig. 3.8 [1].The thermal conductivity was assumed to be constant at 5.64 W/m.k. These constitute relations were imparted in the code to observe the effect on lateral deflection and maximum temperature in the composite

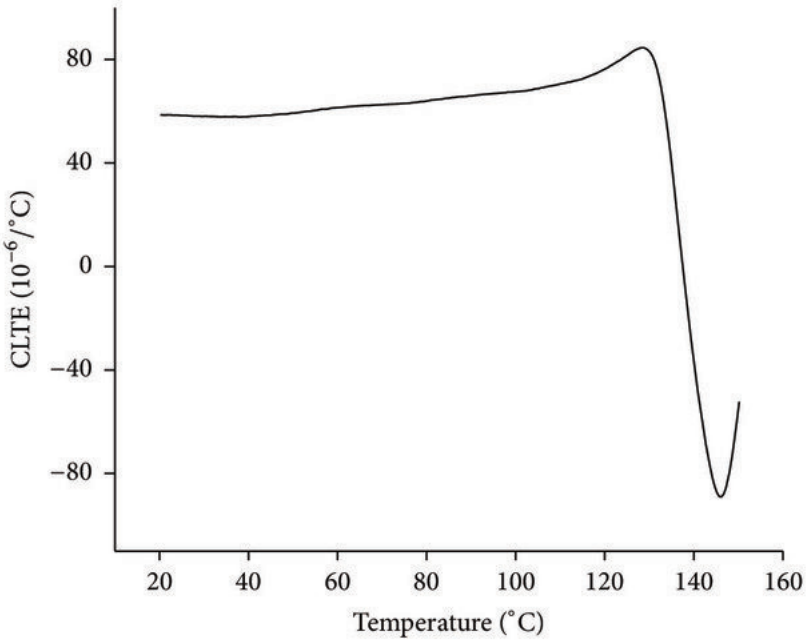

Figure 3.8: Variation of thermal expansion coefficient of epoxy resin at different temperatures [1]

The following properties in the table were used for the FEA simulation

$Temperature(C)$	$E(GPa)$	ν	$\alpha(K^{-1})(\times 10^{-6})$	$K(W/m \cdot K)$
0	62.5	0.3	16.6	5.64
20	61.8	0.3	20.16	5.64
40	61.7	0.305	22.16	5.64
60	61.2	0.31	24.16	5.64
80	60.5	0.315	26.16	5.64

Table 3.2: Mechanical and Thermal Properties of the composite at different temperatures

The results obtained in FEA are shown in Fig.3.9 and 3.10. The plots also verify that

the temperature distribution appears relatively uniform along the spatial axis x at any given time t . Besides deflection is more pronounced in the central region of the micro beam as expected.

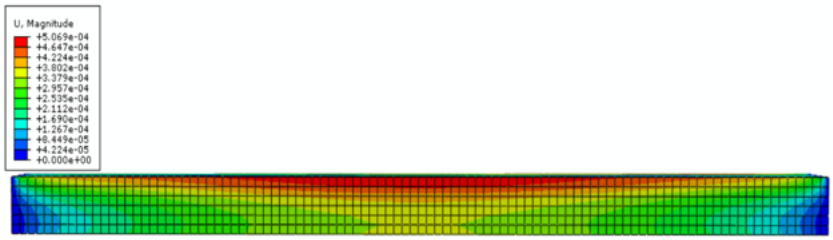

Figure 3.9: Deflection $w(x,t)$ with varying temperature properties at 50 W

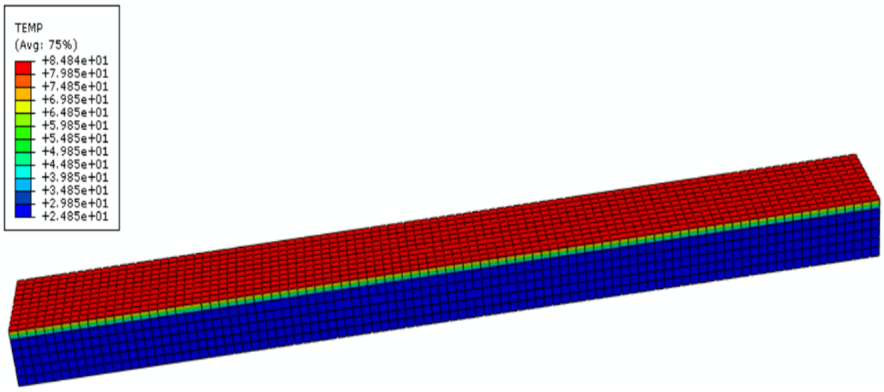

Figure 3.10: Temperature distribution in FEA with varying temperature properties at 50 W

By applying the temeprature dependant eqauations in our analysis we gained a better understanding of how the composite behave at different temperatures. This knowledge is crucial for choosing the right materials for specific uses and ensuring they perform well under expected temperature conditions.

Considering temperature effects during the design process helps us prevent unexpected

problems and make stronger, longer-lasting composite structures. Our research is valuable for industries like aerospace, automotive, and electronics, where temperature changes can affect performance. By understanding how materials respond to temperature, we can develop better solutions to real-world problems.

3.4 Conclusion

In conclusion, our research successfully employed Multiphysics modeling to analyze composites, validating results through Finite Element Analysis (FEA). To conclude we have

- Integrated various physical phenomena into a single model, providing comprehensive insights into composite behavior under diverse operating conditions.
- Demonstrated that increasing input power results in higher maximum temperatures and greater deflection magnitudes in the composite.
- Analyzed the significant role of carbon black in enhancing mechanical strength and thermal conductivity, crucial for robust performance and efficient heat dissipation in challenging environments.
- Emphasized the importance of temperature-dependent mechanical and thermal properties in ensuring the performance, reliability, and longevity of composite materials.
- Highlighted the implications of these properties for structural integrity, thermal management, and functionality, particularly in aerospace applications.
- Provided valuable insights into the intricate interplay between material composition, physical phenomena, and operating conditions, contributing to the design and optimization of composite structures in various industries.

3.5 Future Work

Looking ahead, there are exciting avenues we can explore to build upon our current research efforts. Rather than limiting ourselves to simple structures like the micro bar we analyzed,

we can challenge ourselves with more complex configurations, mirroring real-world applications.

Furthermore, we can introduce more complex approaches by considering point heat sources instead of uniform heat distribution, mimicking the localized thermal conditions encountered in practical scenarios.

Besides we can also expand our model to a thermo-viscoelastic model where the material exhibits both viscous and elastic responses under mechanical loads and also respond to thermal loads.

In essence, our aim is to make our research more relatable and applicable to real-life situations, ensuring that our findings have tangible benefits for various industries. By pushing the boundaries of our understanding and embracing these challenges, we hope to contribute to the advancement of materials science and engineering in a meaningful way.

BIBLIOGRAPHY

[1] Stefano Pandini and Alessandro Pegoretti. Time, temperature, and strain effects on viscoelastic Poisson's ratio of epoxy resins. *Polym. Eng. Sci.*, 48(7):1434–1441, July 2008.

[2] Hongxiao Wang, Xiaohui Zhang, Yugang Duan, and Lingjie Meng. Experimental and Numerical Study of the Interfacial Shear Strength in Carbon Fiber/Epoxy Resin Composite under Thermal Loads. *International Journal of Polymer Science*, 2018, February 2018.

[3] Wurui Ta and Yuanwen Gao. Numerical simulation of the electro-thermo-mechanical behaviors of a high-temperature superconducting cable. *Compos. Struct.*, 192:616–625, May 2018.

[4] ChengSi Lyu, Hao Yu, Juan Jin, WenLong Xu, HanWei Huang, JiaNing Zhang, Quan Wang, JianDong Liu, WeiDong Jiang, He Liu, and HengAn Wu. Multiphysics phase-field modeling for thermal cracking and permeability evolution in oil shale matrix during in-situ conversion process. *Int. J. Rock Mech. Min. Sci.*, 176:105720, April 2024.

[5] Rajneesh Kumar and Richa Vohra. Response of thermoelastic microbeam with double porosity structure due to pulsed laser heating. *Mechanics and Mechanical Engineering*, 23:76 – 85, 2019.

[6] Farshad Shakeriaski, Maryam Ghodrat, Juan Escobedo-Diaz, and Masud Behnia. Recent advances in generalized thermoelasticity theory and the modified models: a review. *J. Comput. Des. Eng.*, 8(1):15–35, January 2021.

[7] Shivanku Chauhan and Rajesh Kumar Bhushan. Improvement in mechanical performance due to hybridization of carbon fiber/epoxy composite with carbon black. *Adv. Compos. Hybrid Mater.*, 1(3):602–611, September 2018.

[8] F. El-Tantawy, K. Kamada, and H. Ohnabe. In situ network structure, electrical and thermal properties of conductive epoxy resin–carbon black composites for electrical heater applications. *Mater. Lett.*, 56(1):112–126, September 2002.

[9] M. Duhovica, P. L'Eplattenierb, I. Caldichouryb, P. Mitschanga, and M. A. Maiera. Advanced 3d finite element simulation of thermoplastic carbon fiber composite induction welding. 2014.

Appendix A

WHERE TO FIND THE FILES

The code can be found in *https* : *//github.com/rohithpremanandan/theisis_code.git*